Transportation Geotechnics 47 (2024) 101265

Contents lists available at ScienceDirect

Transportation Geotechnics

journal homepage: www.elsevier.com/locate/trgeo

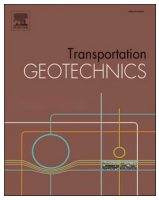

Original Article

Soil mechanics principles for modelling railway track performance

William Powrie

University of Southampton, UK

ARTICLE INFO

Keywords:
Railway track
Settlement
Train passage
Ballast
Principal stress rotation

ABSTRACT

Predicting the performance of railway track is difficult owing to the complex and repeated nature of the loading, the many millions of cycles applied over the life of the structure, the need to characterise the often-infinitesimal rate of accumulation of plastic settlement, and the importance of differential settlements in the along-track direction, which can adversely impact train ride and passenger comfort. These come in addition to the usual soil mechanics challenges of reproducing in a constitutive model the real behaviour of soil and soil-like materials such as railway ballast. Degradation of the geomaterials comprising the trackbed and the underlying ground or earthwork owing to mechanical and environmental effects is a further concern. The paper discusses these issues and explores the application of fundamental soil mechanics principles and advanced constitutive models to understanding and quantifying their effects on railway track and trackbed performance. Recommendations for future research are made.

Introduction

Until at least the advent of high-speed trains in the 1960s, railways were traditionally built on ballast beds laid directly on the earth, often in cuttings or on embankments built from earth. Cuttings and embankments are essential to maintain a railway as close to level as possible. Although less of a problem with today's high-powered electric locomotives, even the largest steam locomotives were not by modern standards very powerful so gradients had to be kept to a minimum. At 1 in 37¾ [1], the Lickey incline between Worcester and Birmingham was considered a severe test for steam and diesel locomotives alike, with long trains, especially freight, needing to be "banked" by additional locomotives pushing at the rear. Thus about 9 500 km (60 %) of the UK railway's ~16 000 railway route km is on embankments or in cuttings [2,3,58]. Many of the world's railways were built in the 1800s or early 1900s, before the discipline of soil mechanics had become established, hence without the benefit of a scientific understanding of soil mechanics principles. Sometimes early earthworks collapsed and had to be rebuilt; or an embankment might simply have gradually settled and been made up back to the original height with whatever material was to hand (often ash residue from the coal burned as fuel in the steam locomotives).

Then until the 1990s, many railway administrations carried out almost all design work in house. This, together with the specialist nature of railway work and a general decline in relative importance of rail transport between the 1960s and 1990s (which meant there was little in the way of new build) might have slowed the integration of soil mechanics principles into many aspects of railway infrastructure engineering. However, the rise in the number of major rail infrastructure projects over the past two decades or so, associated with a global renaissance in rail travel and the need to replace ageing assets and provide resilience to climate change, led to an increased interest in the application of soil mechanics principles to railway geotechnical engineering.

One of the key challenges in railway infrastructure maintenance and management is forecasting the rate at which the track settles as a result of the densification and lateral spreading of the ballast bed and compression of the underlying subgrade. In addition to the usual difficulty of quantifying the evolution of permanent strains under millions of loading cycles, account may need to be taken of the effects of

- trafficking, which may include physical damage to the ballast through grain breakage and attrition
- principal stress rotation and changes in the degree of saturation on the stiffness of the subgrade in cyclic loading, and
- seasonal cycles of shrinkage and swelling due to changes in moisture content on earthwork slopes.

The paper will discuss these issues with reference to recent research carried out at the University of Southampton. It will also consider the nature and role of damping in the response of the trackbed to train passage.

E-mail address: wp@soton.ac.uk.

https://doi.org/10.1016/j.trgeo.2024.101265
Received 23 March 2024; Received in revised form 27 April 2024; Accepted 30 April 2024
Available online 4 May 2024

Forecasting trackbed settlement: Importance and current approach

The ballast that supports the track is a granular material of grain size generally 25–75 mm, which (like the underlying earth) behaves according to soil mechanics principles. As a result of densification and lateral spreading of the ballast, and sometimes settlement of the underlying earthwork, the track gradually settles. Inevitable minor variations in dynamic loading and ground characteristics mean that the track does not settle uniformly but differentially along its length. To restore the track to the desired vertical level, maintenance by raising the track and re-packing the ballast underneath is required from time to time. Historically this process, known as tamping, might have been done by hand, but large machines have been the norm for most routine tamping for many decades.

Tamping is costly in terms of money, carbon and disruption. For example, the UK national infrastructure owner Network Rail typically spends ~£100 M p.a. on tamping and £1 Bn p.a. on track maintenance out of an overall operating budget of ~£10 Bn p.a. In addition to the direct cost, tamping requires substantial investment in plant, the railway is closed to revenue-earning traffic while tamping takes place, and tamping must be planned many months in advance. The ability to forecast rates of railway track settlement with trafficking and over time is thus essential for activities from planning maintenance and route capacity enhancements through to investment decision-making on plant and infrastructure (for example, the robustness of a new or replacement trackform and supporting earthworks). However, track settlement is driven by a complex of interacting mechanisms involving systems and materials from the vehicles through the track and ballast to the subgrade and other support infrastructure. Loading is cyclic, either at relatively high frequency (in the order of cycles per second) from trains or at low frequency (cycles per year) from the environment.

Over the years, many empirical equations for estimating the rate of development of plastic settlement of railway track with train passage have been proposed. Reviews such as those by Dahlberg [4] and Grossoni et al. [5] show that these equations

- do not reproduce the relationships of settlement *vs* number of load cycles seen in the field
- do not reflect current knowledge of the behaviour of soil subgrades and soil-like materials in cyclic loading
- are often critically dependent on the curve fitting parameters used, which in turn depend on the circumstances in which the calibration data were obtained. Hence they do not necessarily reflect the influence of load magnitude or frequency.

A further challenge is that differential settlements, which lead to "long" (in the order of metres) wavelength rail unevenness, are of much greater concern than modest uniform settlements and cannot be predicted without some form of along-track variation. Track engineers associate the accelerated development of track defects with an inadequate track support stiffness. However, the range of acceptable track support stiffness is wide [6] and it is likely that the experiential perception is based on low stiffness being a proxy for plastic settlement potential. Recent work has shown that variations in track level have far more effect on dynamic vehicle load than realistic variations in track support stiffness, as long as a sleeper is not completely unsupported [7,8]. However, it remains to be determined whether even small variations in dynamic load associated with small variations in support stiffness, coupled with small differences in the propensity for the development of plastic settlement, lead through positive feedback to the development of irregular vertical geometry.

Effects of loading magnitude and frequency, principal stress rotation and subgrade soil water content on trackbed response

General response of granular geomaterials to cyclic loading

Powrie et al. [9], summarising the literature including Collins and Boulbibane [10], Suiker and de Borst [11] and Qian et al. [12], list five idealised ways in which a soil or soil-like material subjected to repeated cycles of loading may respond.

1. *Elastic*: strains are proportional to the current applied stress, and are fully reversible in that all of the strain experienced when a load is applied is recovered when the load is removed. There is no cumulative or adverse effect of repeated loading within the elastic loading range.
2. *Elastic shakedown*: plastic (residual or permanent) strains develop during the initial load cycles at a decreasing rate per cycle until a stable elastic state is reached, after which the in-cycle strains are recoverable and no further plastic strain accumulates.
3. *Plastic shakedown*: plastic strains develop during the initial load cycles at a decreasing rate per cycle until a stable state is reached, such that while there is some hysteresis over a cycle no further plastic strain accumulates.
4. *Cyclic creep*: plastic strains develop with every cycle, at a rate that decreases but never quite stops.
5. *Ratcheting*: plastic strains develop with every cycle, but at an increasing rate such that at some point failure or collapse occurs.

A suitable constitutive law for the geomaterials forming the trackbed should be able to reproduce as appropriate any (all) of these five behavioural regimes, in addition to frictional and tensile failure as noted by Suiker and de Borst [11].

Loading frequency

Milne et al. [13] show that a long train (more than about 3 vehicles) applies a spectrum of loading to each sleeper that may be idealised as a complex Fourier series, with loading coefficients at multiples of the car passing frequency (Fig. 1). Generally, as in Fig. 1, the greatest load is applied at the car passing frequency. This should be borne in mind when selecting a loading frequency for laboratory element tests; in most real cases the material response should be quasi-static in that inertial effects (accelerations) should not be significant.

Principal stress rotation

It is well-established that a load on the surface of an elastic bed (half-space) spreads, and the associated stresses reduce, with depth [14]. Thus the zone of influence of a surface load spreads with depth, and an element of soil in the subgrade below the ballast will be subjected to a stress associated with an oncoming or receding train for some time (that is, with the train at some distance) before and after the train has passed directly over it. For a train travelling at constant speed, the vertical normal stress will rise and fall approximately sinusoidally through a maximum when the load is directly above the soil element of interest. This will be accompanied by a horizontal shear stress that rises to a peak while the train is still a short distance away, then reduces through zero when the train is directly above the element of interest to a negative peak before returning to zero as the train recedes. The graph of shear stress against horizontal distance of the train from the soil element of interest has rotational symmetry and is 90° out of phase with the normal stress curve, in the sense that the shear stress is zero when the normal stress is at its peak. The changes in stress to which the soil element is subjected is equivalent to a rotation in the directions of major and minor principal stress [15].

Cyclic changes in the principal stress directions affect the rate of

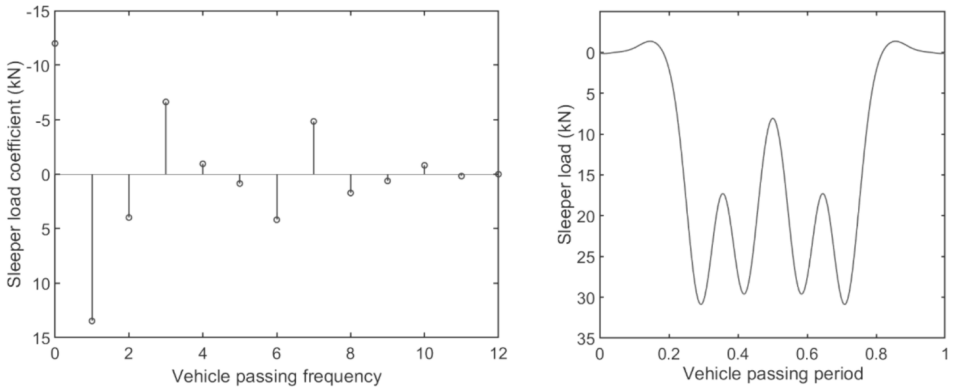

Fig. 1. Loading coefficients (per rail or per sleeper end) for sinusoidal loading at different multiples (harmonics) of the train vehicle passing frequency (a), making up the loading pattern experienced by each sleeper end per vehicle passage (b), for a 65 kN wheel load. Figure: Dr D Milne, from Powrie [54].

accumulation of plastic strains [16–19], albeit to a decreasing extent as the clay content increases [20]. Principal stress rotation may also reduce the saturated resilient modulus of the soil by approximately 20 %–26 %, depending on the overconsolidation ratio (OCR), the clay content, and the way in which the specimen was consolidated prior to cyclic testing [21]. At very shallow depths, principal stress rotation effects are unlikely to be significant because load spreading is minimal. At depth, the changes in stress are small and therefore unlikely to be a concern. Principal stress rotation would be expected to be most significant at depths deep enough for load spreading to have an effect, but not so deep that the stresses have attenuated to negligible values.

Conventional cyclic triaxial testing does not reproduce the changes in shear stress that cause potentially problematic principal stress rotation at modest depths. Cycling the cell pressure as well as the axial stress is possible [22], but does not cause the required principal stress rotation, the results can be counter-intuitive and variations in the extent of membrane penetration can mask changes in specimen volume during the test.

Appropriate principal stress rotations can be approximated reasonably well in the hollow cylinder apparatus, as shown based on numerical analyses by Powrie et al. [23] (Fig. 2).

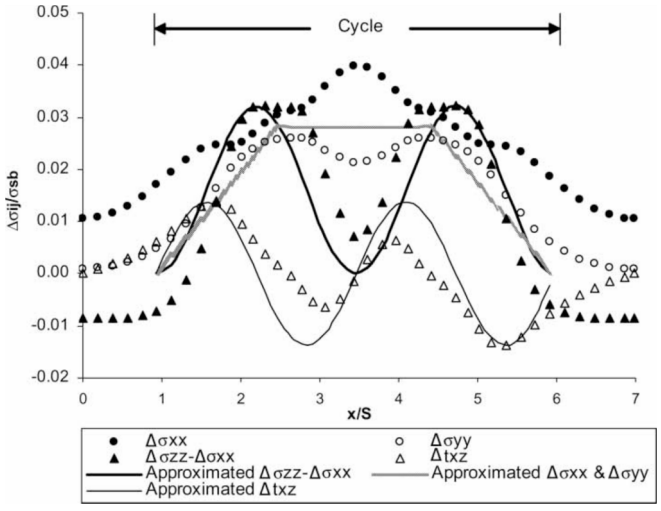

Fig. 2. Stress paths for a soil element at a depth of 1 m below the sleeper soffit during train passage; calculated using dynamic three-dimensional finite element analysis, and approximated in the hollow cylinder apparatus. Figure from Powrie et al. [23].

Ballast response

The ballast layer below the track is typically 300 mm thick. At the surface (immediately below the sleeper soffit), loading is likely to be purely vertical. However, the finite element analyses presented by Powrie et al. [23] and discrete element analyses by Bian et al. [24] indicate that principal stress rotation effects resulting from the movement of the load become significant within the uppermost 300 mm below the track. Testing ballast in a hollow cylinder apparatus would be challenging, owing to the large (typically 30–50 mm) grain size. Also, as pointed out by Powrie et al. [23], the in-situ stress state must be considered in addition to the incremental stresses when assessing the variation in principal stress direction during loading.

For practical reasons, the response of ballast to cyclic loading is usually investigated in large-scale conventional cyclic triaxial tests in which only the axial load is varied. Even then, determining an appropriate testing regime is not straightforward. A typical railway ballast triaxial test specimen is 300 mm diameter × 600 mm in height; twice the depth of a typical ballast bed. The triaxial test set-up does not allow for stress attenuation with depth, as would occur in reality. Further, in the field it is likely that the horizontal stress would increase during vertical loading as the material is to some extent laterally contained. Thus, while the neglect of principal stress rotation during triaxial testing of ballast might be considered to err on the unsafe side, testing at constant cell pressure without any allowance for stress attenuation with depth is likely to be conservative.

It has already been mentioned that the trackbed will experience a loading regime that may be considered to comprise a combination of a cyclic loads of different magnitude at frequencies up to about the tenth harmonic of the car passing frequency (Fig. 3). It is challenging to apply loading at frequencies in excess of about 3 Hz in a large triaxial apparatus. Nonetheless, results of cyclic triaxial tests on specimens of railway ballast at different cell pressures and load frequencies reported by Sun et al. [25] illustrate the dependence of the system response on the stiffness and the frequency of loading. For each cell pressure and loading frequency, Table 1 indicates the peak acceleration a_{max} calculated based on the reported cyclic displacement and frequency, and whether the specimen exhibited plastic shakedown to a stable state at which load cycling continued with no further significant strain (no cell shading), or continuing strain ratcheting to failure (grey cell shading). The acceleration needed to cause ratcheting is generally at least 1 g, and increases with both frequency of loading and with specimen stiffness (confining pressure).

The challenges of the required specimen size mean that compared with most other granular geomaterials, the literature on the triaxial testing of full-size ballast is relatively sparse, especially for very large numbers of load cycles. Abeid et al. (2024) [59] report preliminary results from a series of cyclic triaxial tests on full-size railway ballast,

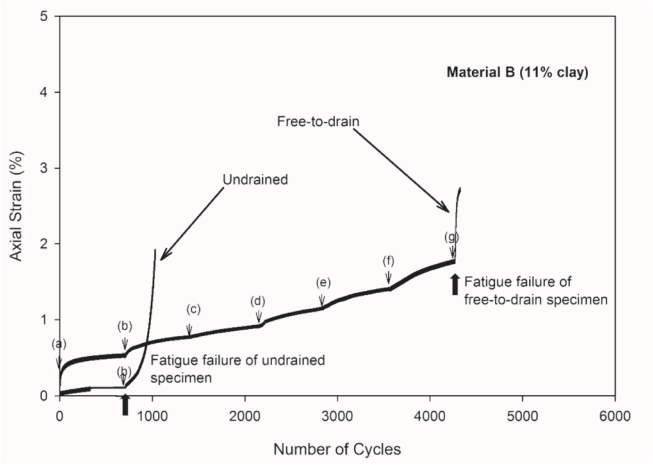

Fig. 3. Response of a simulated railway sub-base material (Material B, 11 % clay content) in undrained and free-to-drain cyclic hollow cylinder tests with principal stress rotation. The letters (a), (b), (c) etc indicate an increase in the magnitude of the cyclic shear stress, which was increased in steps of ± 3 kPa from ±8.5 kPa to a maximum of ±29.5 kPa. Figure from Mamou et al. [31].

Table 1
Maximum accelerations in triaxial tests on ballast specimens at different loading frequencies and cell pressures. Unshaded cells indicate plastic shakedown to a stable state; entries in italics indicate continuing displacements (ratcheting). Data from Sun et al. [25].

	Frequency of loading				
Cell pressure	6 Hz	12 Hz	18 Hz	24 Hz	30 Hz
10 kPa	0.09 g	0.35 g	*0.90 g*	*3.6 g*	*5.0 g*
30 kPa	0.12 g	0.47 g	0.86 g	*2.3 g*	*5.0 g*
60 kPa	0.08 g	0.40 g	0.72 g	1.5 g	*3.6 g*

intended to elicit the primary mechanism of settlement (densification or lateral spreading) and the conditions including stresses and number of load cycles at which significant grain breakage or attrition might first occur. Grain breakage is known to contribute to track settlement, especially on ballast made of more fragile minerals such as limestone [26,27]. Grain breakage seems to be less significant during simulated trafficking for ballast made of tougher minerals such as granite [28,29]. Attrition will still occur, potentially altering the grain form, angularity and surface roughness [30]. Mineralogical analysis indicates that the dust arising during the handling of granite ballast is primarily the relatively soft component mineral feldspar.

Subgrade response

Mamou et al. [31,32] reported the results of cyclic tests on simulated railway subgrade materials of different fines content in a hollow cylinder apparatus from an initial isotropic effective confining stress of 33 kPa. The simulated subgrade materials were designed to be representative of those used on South African heavy haul railways, as used by Gräbe and Clayton [20,21]. Saturated specimens were subjected to cycles of axial stress of 0 to 30 kPa, together with cycles of shear stress at a phase lag of 90°, starting at ± 8.5 kPa and increasing in increments of ±3 kPa. Test were carried out in both undrained and free-to-drain conditions, at a quasi-static load frequency of 30 cycles per hour. The difficulty of relating such tests directly to field conditions, where a loading frequency of 30 cycles per hour might be most representative of the passage of whole trains and the drainage path length would be substantially longer, is discussed by Mamou et al. [31].

Typical results in terms of the accumulation of axial strain with number of loading cycles for Material B, which had a clay content of 11 %, are shown in Fig. 3. Responses of plastic shakedown, cyclic creep and ratcheting to failure (described as "fatigue" on Fig. 3) were observed as the cyclic shear stress increased. Perhaps owing to the magnitude of the initial stress cycle, no purely elastic phase was observed and shakedown was always plastic (that is, the stress cycles always exhibited some hysteresis).

Fig. 4 plots the resilient Young's modulus against the number of load cycles for Material B in (a) undrained and (b) free to drain tests. For these saturated specimens, the magnitude of the shear stress cycle (hence principal stress rotation) seemed to have little effect on the resilient modulus until the value of cyclic shear stress at which failure occurred was reached. The resilient Young's modulus was approximately constant at about 100 MPa in both stable loading episodes in the undrained tests, and gradually increased from about 60 MPa to 100 MPa with number of load cycles in the free-to-drain tests, in a trend seemingly uninfluenced by the changes in the cyclic shear stress magnitude.

Mamou et al. [31] identified cyclic shear stress thresholds in undrained and free-to-drain conditions, which showed an increase with increasing clay content over the range of clay contents tested (Fig. 5). The right-hand vertical axis on Fig. 5 indicates the depth below the sleeper soffit at which each cyclic shear stress magnitude might be experienced, according to the analyses reported by Powrie et al. [23]. In

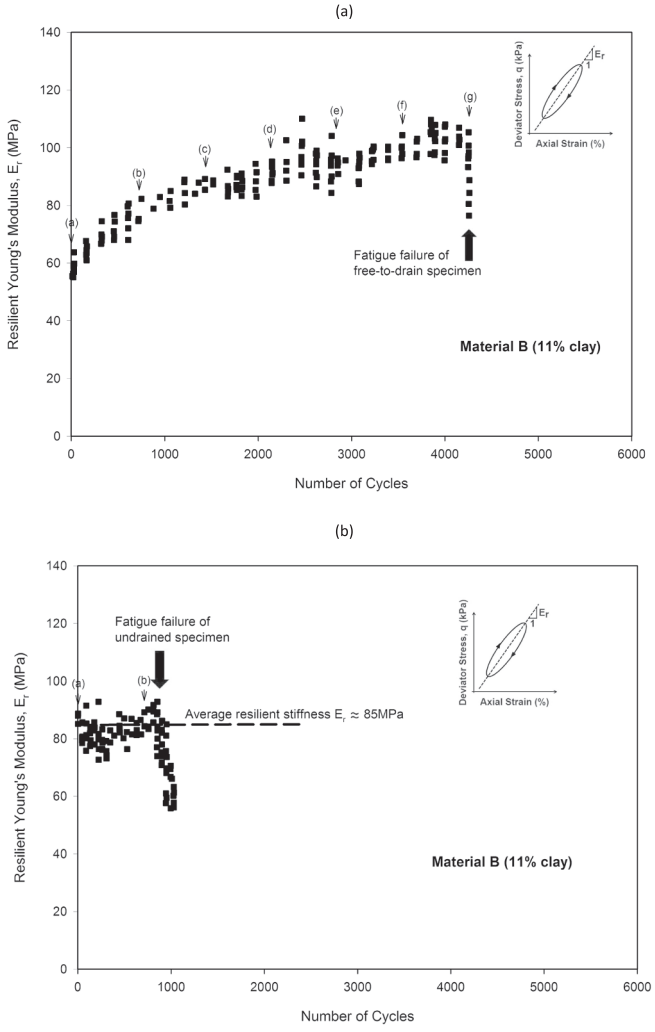

Fig. 4. Change in resilient Young's modulus during shear stress cycling in (a) undrained and (b) free-to-drain cyclic hollow cylinder tests on saturated simulated railway subgrade Material B, 11% clay content. The letters (a), (b), (c) etc indicate an increase in the magnitude of the cyclic shear stress as explained in the caption for Fig. 5. Figures from Mamou et al. [31].

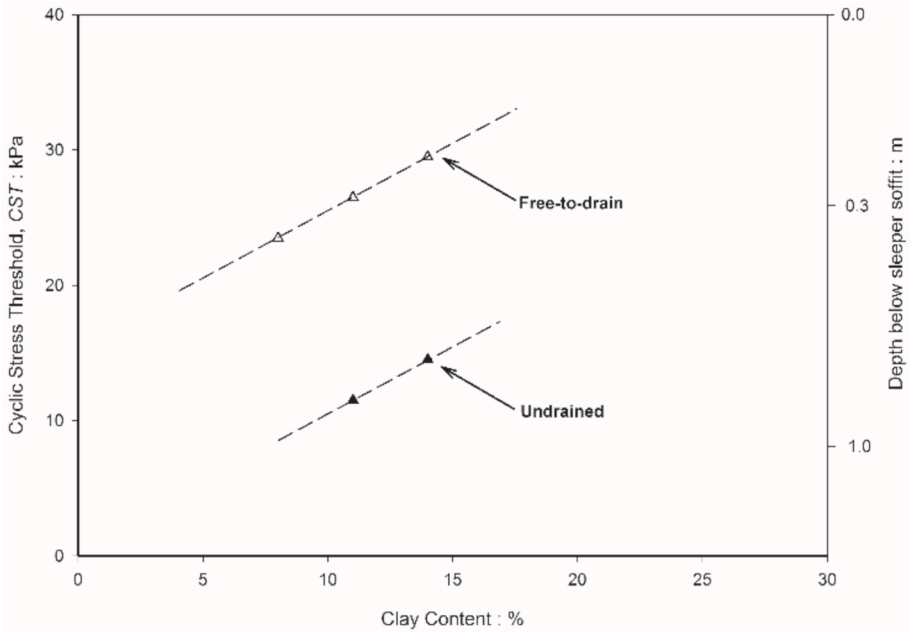

Fig. 5. Cyclic shear stress threshold as a function of material clay content in undrained and free-to-drain conditions. Figure from Mamou et al. [31].

undrained conditions, trackbed materials at depths greater than about 1 m below the sleeper soffit would remain below the cyclic shear stress threshold that would cause failure. In free-to-drain conditions, trackbed materials at all depths below the bottom of the ballast (assuming a ballast depth of 0.3 m) would be remain below the threshold.

Mamou et al. [31] note that in earthquake engineering, it is conventional to identify a threshold cyclic strain beyond which changes in stiffness and (in undrained conditions) pore water pressure start to become significant. Mamou et al. [31] explain their reasons for investigating a threshold stress, which has also been the approach adopted by other researchers in the field (for example [18,33–35]) and indeed was the basis of arguably the first scientific approach to railway trackbed design by Heath et al. [36]. However, the need for Grossoni et al. [5] to make the threshold stress in their track settlement evolution model (discussed below) dependent on stiffness suggests that exploring a threshold strain approach (or at least a stress ratio) might be worthwhile. In a railway context, this remains the subject of ongoing research.

Effect of subgrade moisture content

The tests reported by Mamou et al. [31,32] were on saturated subgrade materials. The effect of unsaturation, and the consequent suction in the soil, was investigated in tests by Blackmore et al. [37] on the simulated subgrade material B as tested by Mamou et al. [31], with a clay content of 11 % by dry weight. They showed that the resilient modulus in free-to-drain conditions increased dramatically from an average of about 40 MPa at a water content of about 8 % to an average of about 550 MPa at a water content of about 4 %, in cyclic triaxial compression tests. (They note that for specimens tested close to saturation at a water content of about 8 %, the resilient moduli measured in the triaxial apparatus were about half the corresponding values measured in pure axial loading in the hollow cylinder test apparatus – that is, without principal stress rotation. They suggest this might have been due to a build-up of pore water pressure in the cyclic triaxial specimens, which were tested at a higher frequency of 0.5 Hz than the frequency of 0.0167 Hz used in the hollow cylinder tests). The variation in free-to-drain resilient modulus with water content measured by Blackmore et al. [37] in free-to-drain cyclic triaxial tests is shown in Fig. 6. For water contents of 5 % or less, Blackmore et al. [37] had some success in relating the suction stresses back-calculated from the

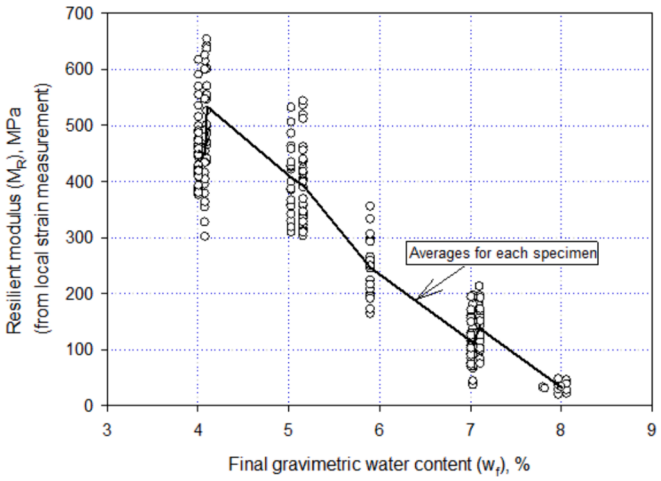

Fig. 6. Variation in free-to-drain resilient modulus with water content in free-to-drain cyclic triaxial tests. Figure from Blackmore et al. [37].

measured values of resilient modulus using the approach described by Heath et al. [38] to the suction stress characteristic curves determined according to Lu and Likos [57] and Lu et al. [39].

Blackmore et al. [37] also investigated the effect of specimen water content on the ratio of the resilient modulus without principal stress rotation to that with principal stress rotation applied. This is shown in Fig. 7.

Blackmore et al. [37] conclude that, while principal stress rotation is significant when the subgrade material is at or close to saturation, its effect on the resilient modulus for unsaturated materials may reasonably be neglected. The reduction in stiffness of near-saturated soils when principal stress rotation is applied could be significant if subgrade materials in some locations (depending on local topography and drainage) become more likely to be saturated in the future, as a result of increased storminess and rainfall intensity associated with climate change.

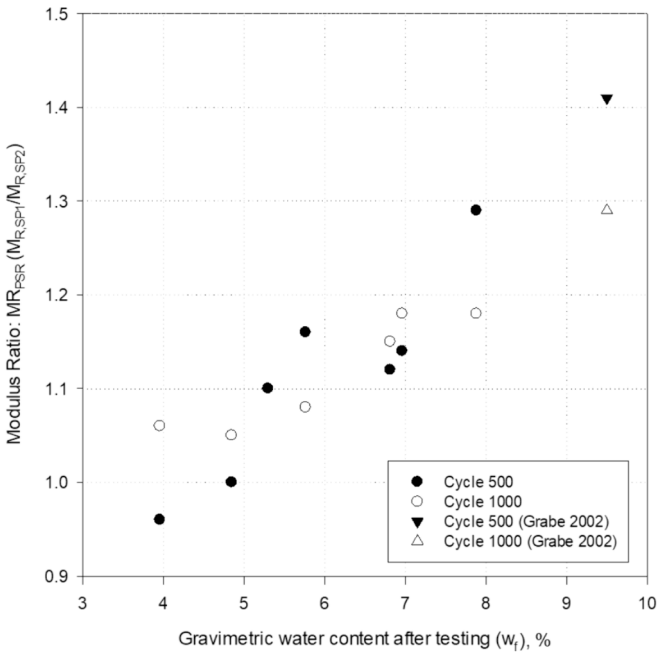

Fig. 7. Effect of principal stress rotation on the resilient modulus M_R at different water contents: resilient modulus ratio (M_R without PSR ÷ M_R in comparable tests with PSR) as a function of specimen water content in hollow cylinder tests. Figure from Blackmore et al. [37].

A Semi-analytical approach to calculating the evolution of track settlement

Research following the Hatfield rail disaster in October 2000 [40] led to a comprehensive understanding of the mechanics of wheel-rail interaction and the development of sophisticated vehicle-track interaction (VTI) analysis programmes. These are based on multi-body mass-spring-damper representations of trains and detailed consideration of the wheel-rail interface, with the trackbed response generally represented as elastic. However, recent developments have seen the incorporation of empirical (for example, [41]) and semi-analytical (for example, [5]) trackbed settlement equations. The semi-analytical approach proposed by Grossoni et al. [5] represents the ballast and subgrade as having elasto-plastic response, in which plastic strains occur above a threshold stress. If the initial threshold stress is exceeded, the maximum previous stress becomes the new threshold stress for subsequent load cycles (Fig. 8).

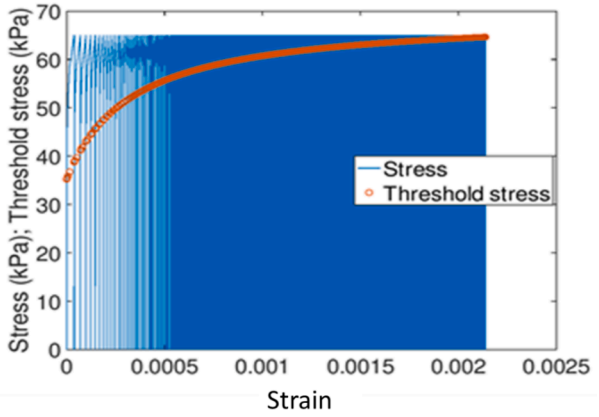

Fig. 8. Typical calculated stress–strain response and evolution of threshold stress in a vehicle-track interaction analysis using the semi-analytical approach of Grossoni et al. [5]: Figure from Grossoni et al. [5].

The threshold stress must be greater for materials of higher stiffness; otherwise, increasing the subgrade stiffness increases the rate of plastic settlement, which is inconsistent with experiential evidence. Calculated plastic strains are used to update the variation in track level along a length of track every 10 000 cycles or so in a vehicle dynamics-based vehicle-track interaction analysis, following the methodology given by Grossini et al (2019) indicated in Fig. 9.

Starting from an initial variation in vertical track geometry based on actual measurements, and using suitable subgrade and vehicle parameters, the approach is shown by Grossoni et al. [5] to give an evolution of mean vertical settlement with number of loading cycles that is within the range calculated using other popular empirical formulae.

This approach, and that described by Nielsen and Li [41], represent a significant advance on a simple reversible linear elastic trackbed model. Coupling a non-reversible trackbed response with the vehicle-track interaction programmes that simulate vehicle dynamic effects in principle enables the effects of train speed (loading frequency) and axle load to be considered, if the influence of these parameters is included in the empirical or semi-analytical settlement equation. The effects of principal stress rotation in the near-surface subgrade soil, or of a change in earthwork or subgrade moisture content and effective stress state associated with vegetation, climate and drainage effects would similarly need to be incorporated into the settlement equation. Reducing track settlement by interventions to the ballast bed or the sleeper-ballast interface are outside the scope of this paper, but some are summarised by Indraratna et al. [42] and Abadi et al. [28,29].

A rheological approach

Ognibene et al. (2022) [60] propose a rheological model for estimating railway track settlement, shown schematically in Fig. 10, in which the rail, sleeper and ballast are represented by masses m_r, m_s and m_b respectively. The railpad between the rail and the sleeper is characterized by a linear Kelvin-Voigt unit having stiffness k_{rp} and damping c_{rp}. The ballast layer is simulated using a bespoke cyclic visco-elastic–-plastic unit, comprising a linear Kelvin-Voigt unit in series with a plastic hardening Iwan-type unit. The Kelvin-Voigt unit is made up of a spring of stiffness k_b in parallel with a viscous dashpot with damping c_b. The plastic-hardening Iwan unit consists of a frictional (dissipative) slider in parallel with two hardening springs, with the frictional element defined

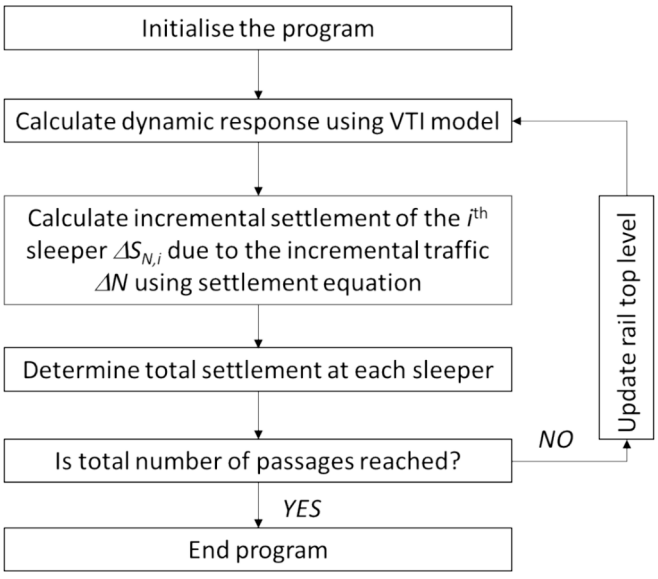

Fig. 9. Flow diagram of the methodology used to update the rail top geometry (level) to account for plastic settlement by Grossoni et al. [5]. Figure redrawn from Grossoni et al. [55].

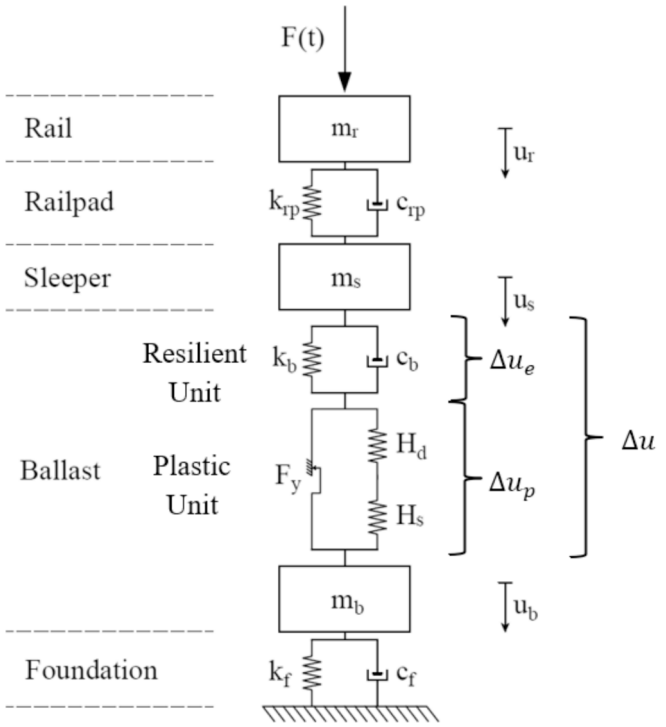

Fig. 10. Rheological model for estimating track settlement. Figure from Ognibene et al. (2022) [60].

by a threshold force F_y and the hardening springs by stiffnesses H_d and H_s. When the force across the ballast F_b is greater than F_y the unit undergoes irreversible (plastic) deformation $(F_b - F_y)/H$ where H is the equivalent stiffness of the hardening unit, $\frac{1}{H} = \left(\frac{1}{H_d} + \frac{1}{H_s}\right)$. The hardening parameters are set to increase exponentially with accumulated plastic settlement. H_d represents plastic settlement due to densification of the ballast and H_s lateral spreading. The threshold force F_y also changes with plastic settlement. There are in total five plastic parameters: the two hardening spring parameters H_d and H_s, and three further parameters that control how these and the threshold stress on the ballast change with plastic settlement. The parameter values can be set so that plastic settlement due to ballast densification governs during the first stages of loading, with settlement due to lateral spreading becoming dominant once the ballast has reached a stable volumetric state. The foundation layer, which is represented by rubber mats in the Southampton Railway Testing Facility used to obtain the data on which the model is based, was characterized by a linear Kelvin-Voigt unit having stiffness k_f and damping c_f. A harmonic force $F(t)$ applied on the top of the rail simulates cyclic wheel loading, and an implicit nonlinear Newmark algorithm is used to solve the resulting system.

With the exception perhaps of the viscous elements for the ballast and a granular subgrade, the rheological elements are intuitive and conform with observed granular material behaviour in terms of the evolution of plastic settlement. (Damping in granular materials would be expected to be frictional rather than viscous, but characterising it in ths way is not well-established). The onset of plastic settlement is still, however, defined by a threshold stress rather than a threshold strain. Ognibene et al. (2022) [60] calibrate the parameters against data from the Southampton Railway Testing Facility at two different axle/wheel loads (98 kN and 157 kN), presented by Abadi et al. [43]. While not a test of the true predictive capability of the model, Ognibene et al (2022) [60] do demonstrate that it is able to differentiate between these tests and calculate curves for loading regimes involving switching between axle load magnitudes (Fig. 11). As found experimentally by Stewart

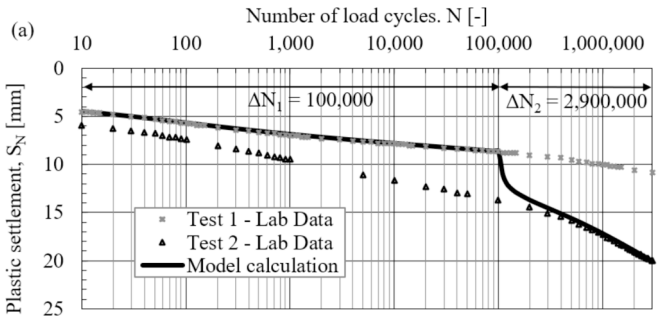

Fig. 11. Use of the Ognibene et al (2022) [60] model to calculate track the evolution of settlement for two different loading scenarios. Figure from Ognibene et al (2022) [60].

[44], the development of plastic strains is heavily influenced by the greatest loads, and on switching from a lower load to a higher load the ballast state quite rapidly moves to a condition that would have obtained had the higher load been applied from the start.

A more rigorous approach

There are soil models (for example, [45,46]) potentially capable of adequately representing the response of geomaterials (clayey and sandy soils) to cyclic loading, reproducing critical state, inherent and stress-induced anisotropy, hysteresis, pore pressure response, hardening and softening, soil structure degradation and threshold stress effects (beyond which a component of strain is permanent). These have been implemented into commercial finite element programs including ABAQUS [47] and PLAXIS [48], enabling 2D and 3D analyses to be conducted both in undrained conditions and with fully coupled solid–fluid interaction using Biot's consolidation theory [49]. Other examples include Zhao et al. [50]. The finite element models can be used to calculate transient and residual stresses, pore water pressures and movements in a section of an earth embankment during simulated train passage. Consolidation is formulated dynamically considering the movements of the solid and the fluid phases and pore water pressures, giving validity for any loading frequency and soil permeability.

Fig. 12 summarises pictorially the 2D coupled finite element analyses carried out by Sang-Iam [47], using the elastoplastic soil model proposed by Zhang et al. [46] implemented as a user-defined element in ABAQUS. The model was modified to account for the effect of Lode angle through an implementation of Matsuoka-Nakai failure criterion [51]. Fig. 12 shows a cross-section of the embankment modelled, a view of the mesh and the sequence of analysis, which involved updating the variables to account for the effects of previous loading cycles. The effect of a moving train was modelled by the application of the dynamic rail loads on a plane slice based on the understanding developed by Milne et al. [13], accounting for out-of-plane load spreading and the flexural rigidity of the rails. The initial overconsolidation ratio of the soil increases from 1 near the point immediately below the trackbed (point A) to 5 at the embankment base (point D). (This is a result of the mesh initialisation process, reflecting the fact that the embankment material has been placed artificially rather than deposited naturally).

Results for the variation with normalised depth y/S (where S is the sleeper length) below the bottom of the trackbed along the track centreline of (a) the increase in pore water pressure Δp_w and (b) the vertical displacement u_y in an embankment of hydraulic conductivity k in response to a single application of a maximum stress at the rail seat R_{max}, applied and removed over a time period consistent with a load moving at a speed $v_T = 10$ m/s, are shown in Fig. 13a and b. These distributions are for the moment in time when the rail seat load is at its maximum. The simulated speed is relatively low owing to computational limitations, as discussed by Sang-Iam [47]. As might be expected, the change in pore water pressure Δp_w increases (for the load speed simulated) as the

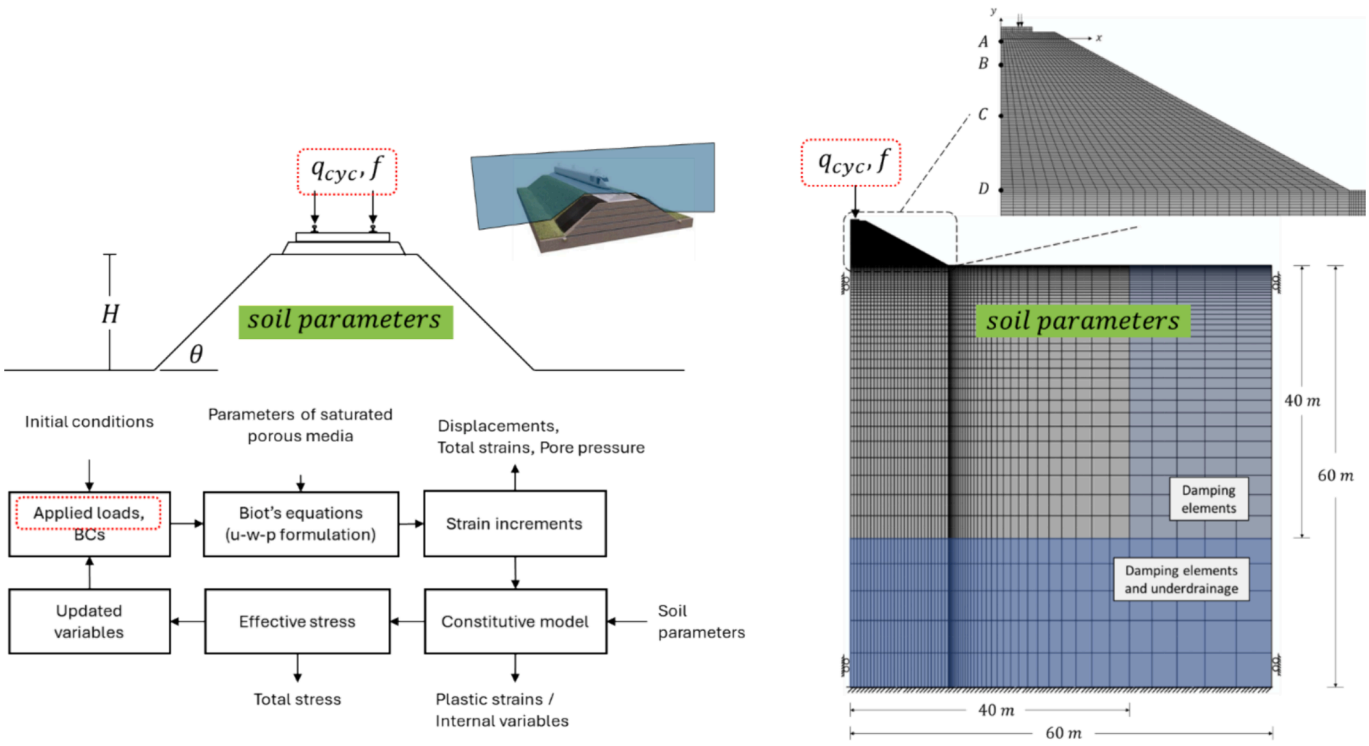

Fig. 12. Schematic representation of 2D finite element analyses of transient loads representative of a moving train carried out by Sang-Iam [47]. Figure from Sang-Iam [47].

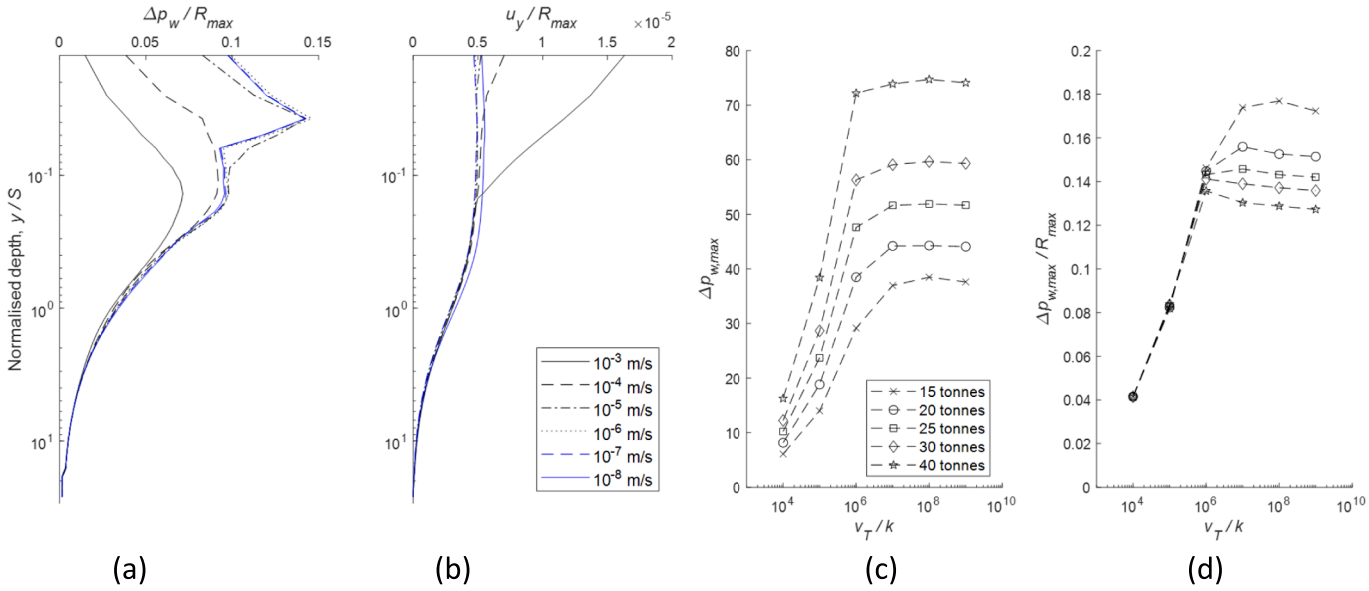

Fig. 13. Variation with normalised depth below the bottom of the trackbed of (a) increase in pore water pressure Δp_w and (b) vertical displacement u_y, both at the centreline of the track in an embankment of hydraulic conductivity k in response to a maximum applied stress at the rail seat R_{max} at a rate corresponding to a single axle load moving at a speed $v_T = 10$ m/s, at the instant of maximum load; (c) shows the maximum increase in pore water pressure at a depth of 0.1 m below the trackbed (Point A) during the period of application of the load, and (d) this maximum increase in pore water pressure normalised by the maximum applied stress at the rail seat, as functions of the simulated load speed v_T divided by the soil hydraulic conductivity k. Figure from Sang-Iam [47].

hydraulic conductivity k reduces towards about 10^{-5} m/s, below which value the soil behaviour is effectively undrained and further reductions in hydraulic conductivity have no impact (Fig. 13a). Fig. 13b shows that a higher hydraulic conductivity leads to a greater vertical displacement over the uppermost 15 cm or so of the embankment, because drainage during loading takes place over this depth owing to the relatively short drainage path length.

Fig. 13c shows the maximum increase in pore water pressure, Δp_w, at a depth of 0.1 m below the trackbed (Point A) during simulated train passage, and Fig. 13d shows this maximum increase in pore water pressure normalised by the maximum applied stress at the rail seat; in both cases as functions of the simulated load speed v_T divided by the soil hydraulic conductivity k. Again as might be expected, the maximum increase in pore water pressure increases with axle load, and also with

increasing V_T/k (reducing hydraulic conductivity k) up V_T/k of about 10^6, above which value, the maximum pore water pressure increase rises only with axle load (Fig. 13c). The fully normalised plot in Fig. 13d shows that when the soil response is almost drained (V_T/k less than about 10^6), the maximum pore water pressure increase varies in proportion with the axle load for a given value of V_T/k. When V_T/k is greater than about 10^6, the maximum increase in pore water pressure is proportionately greater for lower axle loads. This is probably a result of the more plastic response of the soil below the bottom of the trackbed to the increased axle load. The curve in Fig. 13d for the axle load of 15 tonnes is similar to the corresponding curve presented by Bian et al. [52], based on the analysis of a poro-elastic soil under moving train loads.

Fig. 14 shows the distribution with depth below the centre of the track of (a) the residual excess pore water pressure and (b) vertical displacement after the train has passed, and (c) time histories of excess pore water pressure at different depths during the passage of a train comprising 1, 10, 25 and 39 vehicles. The loading represented a train comprising different numbers of FAA bogie low-deck ("well") container wagons of the type built for EWS by Thrall, York (UK) in 1999, having a uniform axle load of 25 tonnes, travelling at a constant speed of 10 m/s over a clay fill embankment with a hydraulic conductivity of 10^{-7} m/s. The results are plotted for soil elements at points A, B, C and D, at depths below the trackbed of 0.10 m, 1.0 m, 3.0 m and 6.0 m respectively. As the train length increases, two competing effects influence the residual pore water pressure at a given depth. The first is the build-up of further excess pore water pressure associated with each wagon, and the second is the additional time available for excess pore water pressure dissipation. At shallow depths (<0.15 m) where the drainage path for excess pore water pressure dissipation is smaller, the second effect (additional time for excess pore water pressure dissipation) dominates. Below about 0.15 m depth, including at the point B (at a depth of 1.0 m), the greater drainage path length enables the excess pore water pressure to build up with each successive wagon passage, so the residual excess pore water pressure increases with train length. At points C and D, the magnitude of the residual excess pore water pressure increases but the over-consolidation ratio of the soil these depths is such that, for the number of wagon passes shown here, it is negative (that is, a suction) owing to the tendency of the soil here to dilate during early-stage shearing. The analysis illustrates the complex of factors influencing the transient soil response below a moving train.

Finally, Fig. 15 shows distributions with depth of (a) residual excess pore water pressure and (b) residual vertical displacement after 1, 3, 10, 30, 60 and 100 passages of a 25-vehicle FAA freight wagon train of 25 tonne axle loads moving at a speed of 10 m/s over an embankment with a hydraulic conductivity of 10^{-7} m/s, and (c) residual excess pore water pressure and (d) residual vertical displacement after 100 train passes for soil hydraulic conductivities of 10^{-5} and 10^{-7} m/s. The time interval between successive trains was 15 min. The build-up in pore water pressure and vertical displacement with number of train passages is clear (Fig. 15a and b), as is the difference between the two values of hydraulic conductivity (Fig. 15c and d). For the higher permeability soil, the residual excess pore water pressure after the trains have passed is effectively zero. For the lower permeability soil, residual excess pore water pressures of up to about 20 kPa remain at a depth of 2–3 m below the bottom of the track bed. The residual displacement over the top 0.4 m or so is greater for the higher permeability soil, because the lower permeability soil has not fully consolidated at the end of the period of train passages.

The finite element model can in principle include the effects of earthwork geometry, soil type, changes in pore water pressures arising from soil permeability, vegetation, weather, climate and drainage effects, and train configuration, axle weight, speed and frequency. However, the computational demand is enormous; hence other, simpler methods of calculation for routine use will be required, such as the high-cycle accumulation models used in offshore engineering (for example, [53]). Further work is also needed to:

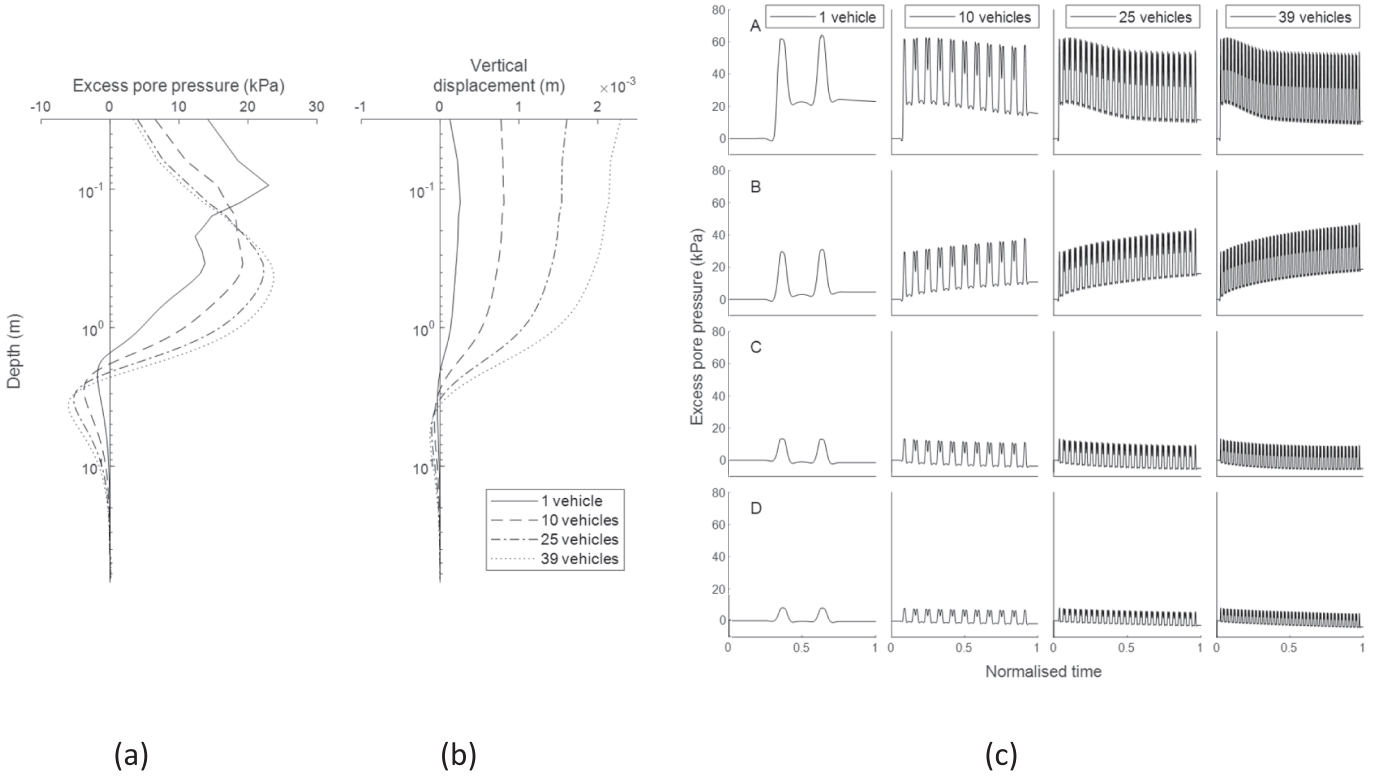

Fig. 14. Calculated distributions with depth of (a) residual excess pore water pressure and (b) residual vertical displacement after train passage; and (c) time histories of excess pore water pressure at different depths during the passage of a train comprising 1, 10, 25 and 39 vehicles. Figure from Sang-Iam [47].

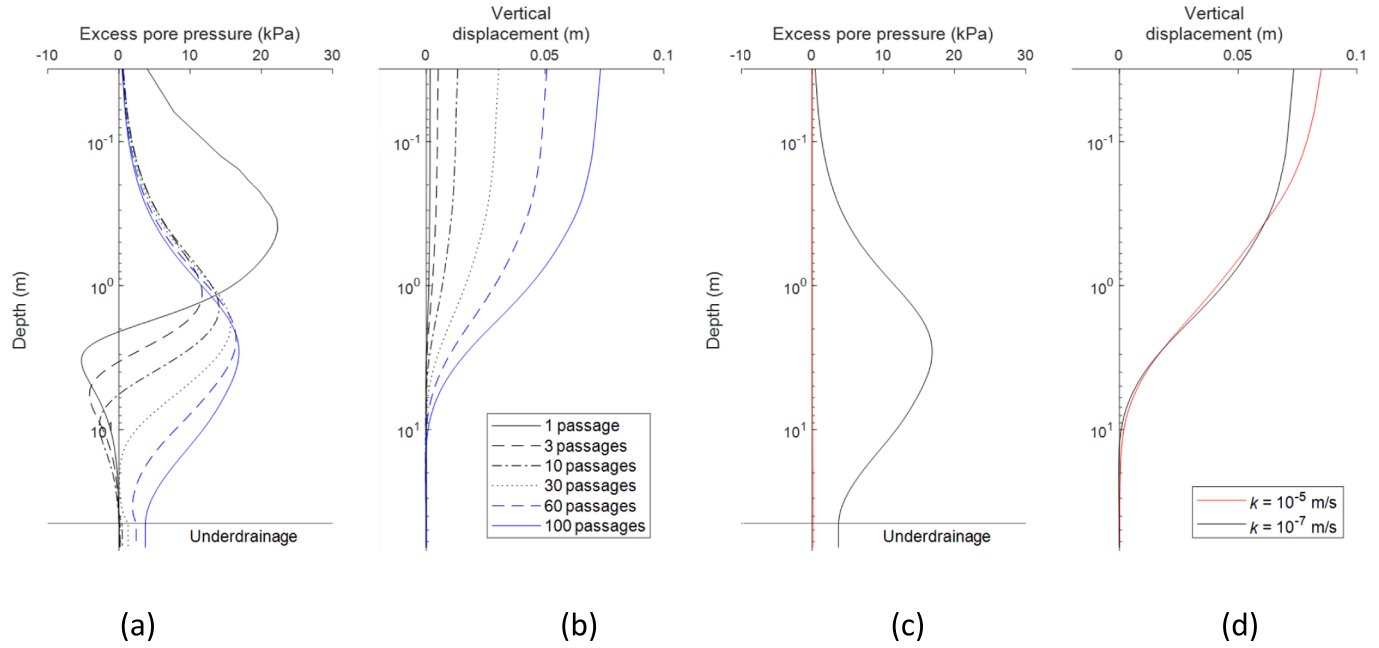

Fig. 15. Distributions with depth of (a) residual excess pore water pressure and (b) plastic vertical displacement after 1, 3, 10, 30, 60 and 100 passes of a 25-vehicle FAA freight wagon with 25-tonne axle loads moving at a speed of 10 m/s over an embankment with a hydraulic conductivity of 10^{-7} m/s, and (c) residual excess pore water pressure and (d) residual vertical displacement after 100 train passes for soil hydraulic conductivities of 10^{-5} and 10^{-7} m/s. Figure from Sang-Iam [47].

- overcome the computational issues limiting the equivalent train speed
- incorporate unsaturated soil behaviour (for modelling the influence of changes in vegetation, climate and drainage conditions)
- determine how to reproduce adequately but realistically the potentially high spatial variability of the trackbed and subgrade; and whether, when and where variations in initial track geometry and dynamic load may be sufficient to drive differences in the evolution of permanent settlements
- validate the model using high quality field data and soils parameters.

The absence of high-quality field data for validation is a weakness of nearly every current railway track settlement model, and is an essential next step if progress is to be made with confidence.

Summary and concluding comments

1. It is useful to be able to forecast the rate of railway track settlement in response to repeated cycles of train loading; but challenging owing to the almost vanishingly small rate of accumulation of plastic settlement per cycle and the unknowability of how conditions will vary along the track.
2. Train loading can usefully be considered as a series of different loads at different frequencies, which for a long train of five or more near-identical vehicles occur at the car passing frequency and integer multiples thereof. The dominant loading as far as track deflection is concerned is likely to be at the car passing frequency.
3. In terms of the stresses experienced by ballast and subgrade materials, train loading may be represented by cycles of increasing then decreasing vertical stress with cycles of horizontal shear stress oscillating about zero, 90° out of phase. This is equivalent to a rotation in the direction of major principal stress during train passage. The combination of load magnitude and principal stress rotation is likely to be potentially most onerous towards the bottom of a 300 mm thick layer of ballast and the top of the underlying subgrade.
4. Element testing of ballast is challenging: the grain size is too big for testing in a hollow cylinder apparatus; the standard height of a large (300 mm diameter) triaxial specimen is, at 600 mm, twice the typical depth of the ballast layer; the triaxial apparatus does not allow for vertical stress attenuation with depth as would happen in the field; and it is uncertain how the in-situ lateral support should be simulated.
5. Subgrade materials tested in conditions of cyclic loading with principal stress rotation exhibit a cyclic threshold shear stress, below which they will shake down plastically to a stable state and above which strains will increase gradually (ratcheting) or accelerate rapidly to failure. The cyclic threshold shear stress is greater in free-to-drain than in undrained loading, and tends to increase with clay content in the range 7–14 %. The resilient modulus for a saturated material could be 20–30 % less with principal stress rotation than without.
6. Unsaturation of the subgrade is important. For an unsaturated material the difference between resilient moduli with and without principal stress rotation becomes much less significant. More importantly, a subgrade with a water content of 4 % could be ten times as stiff as the same material when saturated at a water content of 8 %
7. Semi-empirical, rheological and finite element approaches to estimating the evolution of railway track settlements have been summarised. All show promise but all have disadvantages. The semi-empirical and rheological methods rely on some form of parameter fit or calibration, while the finite element approach is too computationally expensive for routine use. Nonetheless, all offer the potential to be able to account for variations along the track, and in subgrade strength and stiffness as a result of changes in water content resulting from changes in weather / climate, vegetation and drainage condition.
8. The need for research-quality field data to validate any calculation procedure for the evolution of railway track settlement, including more sophisticated models that capture the behaviour of the underlying subgrade and earthwork, cannot be over-stated.

CRediT authorship contribution statement

William Powrie: Writing – review & editing, Writing – original draft, Visualization, Validation, Supervision, Project administration,

Methodology, Funding acquisition, Conceptualization.

Declaration of competing interest

The authors declare the following financial interests/personal relationships which may be considered as potential competing interests: William Powrie reports financial support was provided by Engineering and Physical Sciences Research Council. William Powrie reports financial support was provided by Network Rail Ltd. William Powrie reports financial support was provided by University of Southampton. William Powrie reports financial support was provided by Network Rail (High Speed) Ltd. William Powrie reports financial support was provided by HS2 Ltd. I am on the editorial board of Transportation Geotechnics and serve as a reviewer If there are other authors, they declare that they have no known competing financial interests or personal relationships that could have appeared to influence the work reported in this paper.

Data availability

Data will be made available on request.

Acknowledgements

I am grateful to Rashid Abeid, Letisha Blackmore (née Rorke), Anna Mamou, Giacomo Ognibene and Jeerapat Sang-Iam, on whose doctoral research and dissertations this paper is based; to colleagues Ilaria Grossoni and David Milne for carrying out additional analyses; to co-supervisors Chris Clayton, John Harkness, Louis Le Pen, Jeffrey Priest, Joel Smethurst, David Thompson and Antonis Zervos; and to funders UK Engineering and Physical Sciences Research Council (grants Track 21, EP/H044949 and Track to the Future, EP/M025276) and Network Rail.

References

[1] Anon. BR main line gradient profiles. Hersham, Surrey, UK: Ian Allen Publishing Ltd; 2003.
[2] Briggs KM, Loveridge FA, Glendinning S. Failures in transport infrastructure embankments. Eng Geol 2017;219:107–17. https://doi.org/10.1016/j.enggeo.2016.07.016.
[3] Mair RJ, et al. (2021). *A review of earthworks management.* Network Rail. https://www.networkrail.co.uk/wp-content/uploads/2021/03/Network-Rail-Earthworks-Review-Final-Report.pdf Accessed 24 April 2024.
[4] Dahlberg T. Some railroad settlement models - a critical review. Proc Inst Mech Eng Part F, J Rail Rapid Transit 2001;215(F4):289–300.
[5] Grossoni I, Powrie W, Zervos A, Bezin Y, Le Pen LM. Modelling railway ballasted track settlement in vehicle-track interaction analysis. Transp Geotech 2021;26:100433.
[6] Powrie W, Le Pen L M and the Track Stiffness Working Group (2016). *A Guide to track stiffness* (53pp). Southampton: University of Southampton. ISBN 9780854329946 (also available at https://www.thepwi.org/knowledge/a-guide-to-track-stiffness/).
[7] Milne DR, Harkness J, Le Pen L, Powrie W. The influence of variation in track level and support system stiffness over longer lengths of track on track performance and vehicle track interaction. Veh Syst Dyn 2019;59(2):245–68. https://doi.org/10.1080/00423114.2019.1677920.
[8] Powrie W, Le Pen LM, Milne DR, Watson GVR, Harkness J. Behaviour of under-track crossings on ballasted railways. Transp Geotech 2019;21:100258. https://doi.org/10.1016/j.trgeo.2019.100258.
[9] Powrie W, Le Pen LM, Milne DR, Thompson DJ. Train loading effects in railway geotechnical engineering: ground response, analysis, measurement and interpretation. Transp Geotech 2019;21:100261. https://doi.org/10.1016/j.trgeo.2019.100261.
[10] Collins IF, Boulbibane M. Geomechanical analysis of unbound pavements based on shakedown theory. ASCE J Geotechn Geoenviron Eng 2000;126(1):50–9.
[11] Suiker ASJ, de Borst R. A numerical model for the cyclic deterioration of railway tracks. Int J Numer Meth Eng 2003;57(4):441–70.
[12] Qian J-G, Wang Y-G, Yin Z-Y, Huang M-S. Experimental identification of plastic shakedown behavior of saturated clay subjected to traffic loading with principal stress rotation. Eng Geol 2016;214:29–42. https://doi.org/10.1016/j.enggeo.2016.09.012.
[13] Milne DR, Le Pen LM, Thompson DJ, Powrie W. Properties of train load frequencies and their applications. J Sound Vib 2017;397:123–40. https://doi.org/10.1016/j.jsv.2017.03.006.
[14] Boussinesq J. Applications des potentiels à l'étude de l'équilibre et du movement des solides élastques (Potential applications of the study of the equilibrium and movement of elastic solids). Paris, France: Gauthier-Villars; 1885.
[15] Brown SF. Soil mechanics in pavement engineering. Géotechnique 1996;46(3):383–426. https://doi.org/10.1680/geot.1996.46.3.383.
[16] Chan FWK, Brown SF (1994). Significance of principal stress rotation in pavements. In *Proceedings of the 13th International Conference on Soil Mechanics and Foundation Engineering*, New Delhi, India, 5–10 January 1994, 1823-1826. Taylor and Francis, New York.
[17] Cai Y, Sun Q, Guo L, Juang CH, Wang J. Permanent deformation characteristics of saturated sand under cyclic loading. Can Geotech J 2015;52(6):795–807. https://doi.org/10.1139/cgj-2014-0341.
[18] Guo L, Cai Y, Jardine RJ, Yang Z, Wang J. Undrained behaviour of intact soft clay under cyclic paths that match vehicle loading conditions. Can Geotech J 2018;55(1):90–106. https://doi.org/10.1139/cgj-2016-0636.
[19] Qian J-G, Du Z, Lu X, Gu X, Huang M-S. Effects of principal stress rotation on stress-strain behaviors of saturated clay under traffic-load-induced stress path. Soils Found 2019;59(1):41–55.
[20] Gräbe PJ, Clayton CRI. Effects of principal stress rotation on permanent deformation in rail track foundations. ASCE J Geotechn Geoenviron Eng 2009;135(4):555–65. https://doi.org/10.1061/(ASCE)1090-0241(2009)135:4(555).
[21] Gräbe PJ, Clayton CRI. Effects of principal stress rotation on resilient behavior in rail track foundations. ASCE J Geotechn Geoenviron Eng 2014;140(2):1–10. https://doi.org/10.1061/(ASCE)GT.1943-5606.0001023.
[22] Aingaran S. Experimental investigation of static and cyclic behaviour of scaled railway ballast and the effect of stress reversal. UK: University of Southampton; 2014. PhD dissertation.
[23] Powrie W, Yang LA, Clayton CRI. Stress changes in the ground below ballasted railway track during train passage. Proc Inst Mech Eng Part F: J Rail Rapid Transit 2007;221(2):247–61. https://doi.org/10.1243/0954409JRRT95.
[24] Bian X, Li W, Qian Y, Tutumluer E. Analysing the effect of principal stress rotation on railway track settlement by discrete element method. Géotechnique 2020;70(9):803–21. https://doi.org/10.1680/jgeot.18.P.368.
[25] Sun Q, Indraratna B, Ngo NT. Effect of increase in load and frequency on the resilience of railway ballast. Géotechnique 2018;69(9):833–40. https://doi.org/10.1680/jgeot.17.P.302.
[26] Lackenby J, Indraratna B, McDowell GR, Christie D. Effect of confining pressure on ballast degradation and deformation under cyclic triaxial loading. Géotechnique 2007;57(6):527–36. https://doi.org/10.1680/geot.2007.57.6.527.
[27] Indraratna B, Ngo T, Rujikiatkamjorn C. Performance of ballast influenced by deformation and degradation: laboratory testing and numerical modelling. Int J Geomech 2019;20(1). https://doi.org/10.1061/(ASCE)GM.1943-5622.0001515.
[28] Abadi TC, Le Pen L, Zervos A, Powrie W. Improving the performance of railway track through ballast interventions. Proc Inst Mech Eng Part F, J Rail Rapid Transit 2018;232(2):337–55.
[29] Abadi TC, Le Pen L, Zervos A, Powrie W. The effect of sleeper interventions on railway track performance. ASCE J Geotechn Geoenviron Eng 2019;145(4):1–14.
[30] Gupta A, Madhusudhan BN, Zervos A, Powrie W, Harkness J, Le Pen LM. Grain characterisation of fresh and used railway ballast. Granul Matter 2022;24:96. https://doi.org/10.1007/s10035-022-01263-1.
[31] Mamou A, Powrie W, Priest JA, Clayton CRI. The effects of drainage on the behaviour of railway track foundation materials during cyclic loading. Géotechnique 2017;67(10):845–54.
[32] Mamou A, Priest JA, Clayton CRI, Powrie W. Behaviour of saturated railway track foundation materials during undrained cyclic loading. Can Geotech J 2018;55:689–97.
[33] Cai YQ, Guo L, Jardine RJ, Yang ZX, Wang J. Stress–strain response of soft clay to traffic loading. Géotechnique 2017;67(5):446–51.
[34] Nguyen TT, Indraratna B, Singh M. Dynamic parameters of subgrade soils prone to mud pumping considering the influence of kaolin content and the cyclic stress ratio. Transp Geotech 2021;29:100581.
[35] Toyota H, Takada S. Settlement assessment of sand subjected to cyclic stress related to a load moving over a surface using hollow cylindrical torsional shear apparatus. Transp Geotech 2021;29:100580.
[36] Heath DL, Shenton MJ, Sparrow RW, Waters JM. Design of conventional rail track foundations. Proc Inst Civ Eng 1972;51:251–67.
[37] Blackmore L, Clayton CRI, Powrie W, Priest JA, Otter L. Saturation and its effect on the resilient modulus of a pavement formation material. Géotechnique 2020;70(4):292–302. https://doi.org/10.1680/jgeot.18.P.053.
[38] Heath AC, Pestana JM, Harvey JT, Bejarano MO. Normalizing behaviour of unsaturated granular pavement materials. ASCE J Geotechn Geoenviron Eng 2004;130(9):896–904.
[39] Lu N, Godt JW, Wu DT. A closed-form equation for effective stress in unsaturated soil. Water Resour Res 2010;46(5):W05515. https://doi.org/10.1029/2009WR008646.
[40] UK Office of Rail Regulation. Train derailment at Hatfield: A Final Report by the Independent Investigation Board. London, UK: Office of Rail Regulation; 2006 (accessed March 8 2024).
[41] Nielsen JC, Li X. Railway track geometry degradation due to differential settlement of ballast/subgrade – numerical prediction by an iterative procedure. J Sound Vib 2018;412:441–56.
[42] Indraratna B, Sun Q, Ngo T, Rujikiatkamjorn C. Current research into ballasted rail tracks: model tests and their practical implications. Aust J Struct Eng 2017:1–17.
[43] Abadi TC, Le Pen LM, Zervos A, Powrie W. A review and evaluation of ballast settlement models using results from the Southampton Railway testing Facility (SRTF). Procedia Eng 2016;143:999–1006. https://doi.org/10.1016/j.proeng.2016.06.089.
[44] Stewart HE. Permanent strains from cyclic variable-amplitude loadings. ASCE J Geotechn Eng 1986;112:646–60.

[45] Zhao J, Sheng D, Rouainia M, Sloane SW. Explicit stress integration of complex soil models. Int J Numer Anal Meth Geomech 2005;29(12):1209–29. https://doi.org/10.1002/nag.456.
[46] Zhang F, Ye B, Noda T, Nakano M, Nakai K. Explanation of cyclic mobility of soils: approach by stress-induced anisotropy. Soils Found 2007;47(4):635–48.
[47] Sang-Iam J. Modelling old railway embankments under different traffic conditions. UK: University of Southampton; 2022. PhD dissertation.
[48] Rouainia M, Gaetano E, Panayides S, Scott P. Nonlinear finite-element prediction of the performance of a deep excavation in Boston Blue Clay. ASCE J Geotech Geoenviron Eng 2017;143(5). https://doi.org/10.1061/(ASCE)GT.1943-5606.0001650.
[49] Biot MA. Theory of propagation of elastic waves in a fluid-saturated porous solid II: higher frequency range. J Acoust Soc Am 1956;28(2):179–91.
[50] Zhao HY, Indraratna B, Ngo T. Numerical simulation of the effect of moving loads on saturated subgrade soil. Comput Geotech 2021;131:103930.
[51] Matsuoka H, Nakai T. Stress-deformation and strength characteristics of soil under three different principal stresses. Proc Jpn Soc Civ Eng 1974;232:59–70.
[52] Bian X, Hu J, Thompson D, Powrie W. Pore pressure generation in a poro-elastic soil under moving train loads. Soil Dyn Earthq Eng 2019;125:1–15. https://doi.org/10.1016/j.soildyn.2019.105711.
[53] Niemunis A, Wichtmann T, Triantafyllidis Th. A high-cycle accumulation model for sand. Comput Geotech 2005;32:245–63.
[54] Powrie W (2024). Railway track substructure: recent research and future directions. 3rd ISSMGE Ralph Roscoe Proctor Honor Lecture. Accepted for publication in *Transportation Geotechnics*.
[55] Grossoni I, Andrade A, Bezin Y, Neves S. The role of track stiffness and its spatial variability on long-term track quality deterioration. Proc Inst Mech Eng Part F: J Rail Rapid Transit 2019;233(1):16–32.
[57] Lu N, Likos WJ. Suction stress characteristic curve for unsaturated soil. ASCE J Geotechn Geoenviron Eng 2006;132(2):131–42.
[58] Office of Rail and Road (2021). *Rail infrastructure and assets 2020-2021*. https://dataportal.orr.gov.uk/media/2014/rail-infrastructure-assets-2020-21.pdf Accessed 24 April 2024.
[59] Abeid R S, Murthy M, Abadi T C, Milne D R, Smethurst J A and Powrie W (2024). Triaxial tests to assess the effects of densification, lateral spreading and grain breakage on settlement behaviour of full-size railway ballast. *Proceedings of the 5th International Conference on Transportation Geotechnics*, Sydney, Australia, November 2024.
[60] Ognibene G, Le Pen L, Harkness J, Zervos A, Powrie W. Al-Qadi I and Qamhia 2022;I),:99–112. https://doi.org/10.1007/978-3-030-77234-5_9.

Further reading

[56] Liu C, Thompson DJ, Griffin MJ, Entezami M. Effect of train speed and track geometry on the ride comfort in high-speed railways based on ISO 2631-1. Proc Inst Mech Eng Part F: J Rail Rapid Transit 2020;234(7):765–78. https://doi.org/10.1177/0954409719868050.